

## Modelling and Estimation on Vibration and Noise Level of the Dynamic Wiper System using Input Shaping Strategy

Mohd Azli Salim<sup>1,2,3,\*</sup>, Adzni Md. Saad<sup>1,3</sup>, Chonlatee Photong<sup>4</sup>, Mohd Zarhamdy Md. Zain<sup>5</sup>, Abd Rahim Abu Bakar<sup>5</sup>, Norbazlan Mohd Yusof<sup>6</sup> and Mohd Zaid Akop<sup>1</sup>

<sup>1</sup>Fakulti Kejuruteraan Mekanikal, Universiti Teknikal Malaysia Melaka, Hang Tuah Jaya, 76100 Durian Tunggal, Melaka, Malaysia

<sup>2</sup>Advanced Manufacturing Centre, Universiti Teknikal Malaysia Melaka, Hang Tuah Jaya, 76100 Durian Tunggal, Melaka, Malaysia

<sup>3</sup>Intelligent Engineering Technology Services Sdn. Bhd., No. 1, Jalan TU43, Taman Tasik Utama, 76450 Ayer Keroh, Melaka, Malaysia

<sup>4</sup>Graduate School, Mahasarakham University, Khamriang Sub-District, Kantarawichai District, Maha Sarakham 44150, Thailand

<sup>5</sup>Sekolah Kejuruteraan Mekanikal, Fakulti Kejuruteraan, Universiti Teknologi Malaysia, Jalan Universiti Skudai, 80990 Johor Bahru, Johor Darul Takzim, Malaysia

<sup>6</sup>Centre of Excellence, Projek Lebuhraya Usahasama Berhad, Menara Korporat, Persada PLUS, Persimpangan Bertingkat Subang, KM 15, Lebuhraya Baru Lembah Klang, 47301 Petaling Jaya, Selangor Darul Ehsan, Malaysia

### ABSTRACT

*During wiping operation to wipe rain and dirt out from the windscreen, the wiper generates unwanted noise and vibration. This may cause dissatisfaction to the automotive vehicles due to annoying sounds and perhaps leads to poor visibility to the driver. Therefore, this paper proposes an approach to reduce and eliminate noise and vibration in a windscreen automotive vehicles wiper system. A two-dimensional mathematical model available in the open literature is adopted and integrated with a proposed control scheme, i.e. input shaping. Firstly, analysis is performed based on an original model, i.e. without input shaping in order to determine the noise (frequency) and vibration (amplitude) levels. Comparison is also made between the prediction results with finite element results. It is found that the correlation is reasonably close. The next stage is to introduce the two-impulse input shaping scheme. It is found that the input shaping could reduce certain amount of vibration level. Finally, parametric studies are also performed to examine the effectiveness of the proposed approach.*

**Keywords:** Wiper system, input shaping, vibration level, noise measurement

### 1. INTRODUCTION

Noise and vibration have become increasingly important factors in vehicle design as a result of the quest for increased refinement. There are various sources of noise and vibration typically occurred in the vehicle and windscreen wiper noise is one of them. Additionally, the issue of comfort in automotive cars has become a compulsory factor to indicate the quality of a car [1]. Wiper system is a one of the problem that can create the uncomfortable situation for the driver and passengers. Reducing or eliminating the unwanted noise and vibration created by wiper system becomes more important factor to provide a leading edge in the market to retail the vehicle (Goto et al., 2001). The researches in wiper system attempt in identifying the techniques to decrease or reduce the level of unwanted noise and vibration. The main focus of solving the problem is improving the mechanism of the system.

The first wiper was developed in 1903 by J.H. Apjohn [2]. This inventor came out with a method of moving two brushes up and down on a vertical glass plate. In the same year, this method was

---

\*Corresponding Author: azli@utem.edu.my

enhanced by Mary Anderson where the two brushes were applied on a car in which creating a device that appears to be like a swinging arm, sweeping rain off the windshield. This augmented method was firstly introduced in United States and in 1913 this pattern was improvised until the pattern became a standard feature of all American cars in year 1916. In April 1911, Sloan & Lloyd Barnes registered the first pattern of windshield wiper at Liverpool, England [3]. This first pattern was credited by Jozef Hofmann, the world famous pianist and Mills Munitions. This pattern is continuously improved and in 1919 William M. Folberth produced a pattern for automatic windscreen wiper apparatus. After 3 years, this pattern was granted safe to be used. This prototype of Folberth was recognized as the first automatic mechanism of wiper [1-3].

Late 1950s was the era of improvement for the pattern of wiper and during this time, the improvement focused on perfecting the operation of the wiper itself. The usage of wiper for modern vehicles has become one of the required system. The operating of the wipers had been automated when the washer button was pressed by the driver. This is considered as a major accomplishment as before this the operation of the wipers requires manual procedures to turn it on. In 1969, Robert Kearns introduced the first intermittent wipers where it can operate by using an adjustable time delay. The objective of this idea is to make it possible to select a degree and location of wiping action when the driver needs to clean the windscreen [4].

Saab Automobile introduced headlight wipers across the product range in 1970 [3,5]. This headlight wiper operated on a horizontal reciprocating mechanism by using a single motor. This company concluded that every single motor can only be used at each headlamp only during an action of wiper mechanism. In March 1970, Citroen Company introduced a rain sensitive intermittent windscreen wiper on their models. This was an intelligent method where it only operated during raining condition. This pattern worked in relatively dry condition; when it dries the wiper motor grew a high current. It can defer a device to delay the next wipe for longest time. In wet condition, the current was decreased and thus minimizing the delay time, consequently shorten the time taken to wipe [1,4].

Wiper system has become a necessity equipment in the vehicle but it has a potential to generate unwanted noise and vibration. The noise and vibration of wiper system can be classified into three parts. Squeal or squeaky noise can occur at high frequency range which is up to 1000 Hz, chattering or beep noise occurs at low frequency range of 100 Hz or less and finally reversal noise for frequency range between 100 to 500 Hz. All these types of noise have a potential to cause visual and audible annoyance to driver and passengers during raining condition [6-11].

Various approaches have been actively used to investigate the noise and vibration of the windscreen wiper system which include analytical, numerical and experimental approaches. Okura et.al developed a 2D and 3D mathematical models to investigate blade reversal noise in a wiper system [1,12]. By simulating the models in various conditions, it was found that the reaction force of the wiper blade could be reduced by using a small neck angle or a large neck rotational spring. Furthermore, the study also showed that the arm head twist angle could prevent blade lift during high speed operation.

Contact pressure distribution of the wiper blade using numerical and experimental approaches had been studied by Granouillat and Leblanc [4]. It was found that the predicted contact pressure for various arm loads were very close to the measured data. It can be observed that the higher the arm force produced higher contact pressure along the blade. Goto et.al studied wiper blade squeal noise by using experimental approach [6, 13-14]. Finite element model was developed and the predicted results were used to deduce the equation of motions. The derived equations were then used to identify which parameters were sensitive to squeal noise. They found that damping, friction, surface treatment, neck thickness were the parameters that could reduce squeal noise. In another study they proposed the material and design aspects that could help to reduce squeal noise [15]. Apart from modifying wiper material and design, Chang with

Chang and Stallaert proposed dither control to suppress squeal noise in the windscreen wiper. They found that, through experimental results, wiper squeal can effectively be suppressed by the dither control [8-9, 16-17].

In addition, PSV Wipers Ltd company based in England have developed a grade military specific wipers blades specifically for flat armoured glass. The range of military vehicle equipment around the world consists of high quality extremely robust of wiper system including blades, arm, linkages equipment, control system and many more. It is very important to solve because military vehicle used for defence and national strategy.


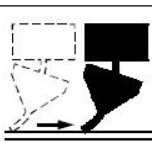

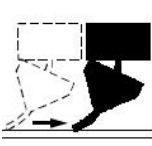

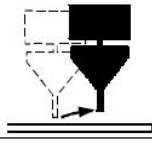
This study developed the modelling estimation and prediction on wiper blade. Then, the governing equation of motion for wiper blade was modelled and the baseline results on vibration response was examined, and verified by using finite element method. Vibration control scheme namely input shaping was implemented into the governing equation, and finally the baseline results had improved in vibration amplitude. At the end of the study, parametric analysis study was taken into the account with current governing equation. Based on the study, the level of unwanted noise and vibration in wiper blade system was slightly decreased, by comparing the results from the baseline.

## 2. MATERIAL AND METHODS

### 2.1 Modelling and Prediction Preparations

In order to simulate the various dynamic characteristics of a automotive vehicles wiper system, modelling estimation and prediction on wiper blade model which includes a complete 2D model is developed [1]. There are five rubber conditions in this model and non-contact are shown in Table 1.

**Table 1** Rubber condition [1]

Condition	C Stick condition between the blade lips on the windshield	D Slip condition	Variable
<b>A</b> Non-contact between the rubber shoulder and the rubber head			$y_A, \theta_a$
<b>B</b> Non-contact condition			$y_A, \delta_c$
<b>JUMP</b> A jump condition between the rubber blade and windshield			$y_A$

In this study, the AC blade condition where non-contact condition between the rubber shoulders with the rubber head and stick condition between the blade lips on the windshield of

automotive vehicles wiper system was chosen. Figure 1 shows the 2D spring-mass model for arm and blade wiper system.

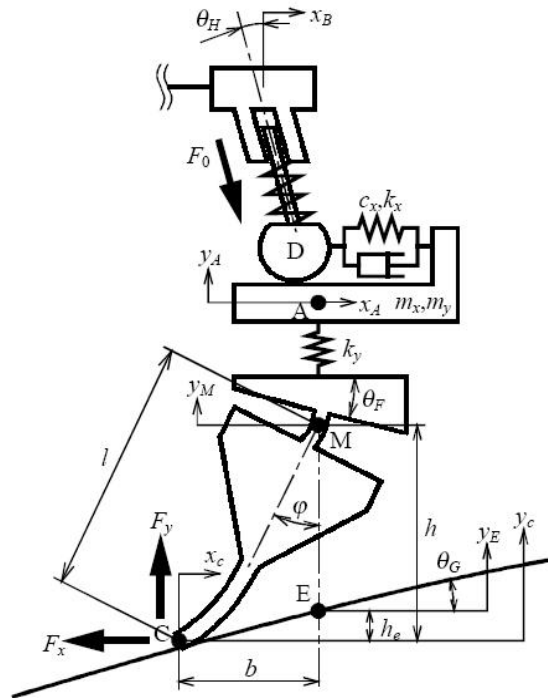


Figure 1. The 2D spring-mass model for wiper system [1]

According to the AC condition, the force is acting at the y-direction. The centre of the rotation located at point  $M_r$  and the length of rubber is denoted by  $l$  with the equation can be expressed as (Okura et al., 2000; Goto et al., 2001)

$$l = \frac{l_a}{2} + l_b + l_c \quad (1)$$

The reaction force,  $P$  is occurred by the deformation of rubber blade,  $\delta_c$  and the equation can be represented as

$$P = \frac{k_a \theta_a}{l} = k_c \delta_c \quad (2)$$

The relationship between reaction force,  $P$  force at x-direction,  $F_x$  and force at y-direction,  $F_y$  can be written as

$$F_x \cos \varphi + F_y \sin \varphi = P \quad (3)$$

where  $\varphi = \theta_a + \theta_F$

Equation (3) is homogeneous, where some assumptions are made; (i) the arm is twisted as a rigid body motion, and (ii) condition D is without mass and slippery without friction, and does not leave the horizontal plane of the top arm. The origin for x-direction is located at  $y_A$  and  $y_M$ . Point M is  $\theta_A = \delta_c = 0$  and  $x_A = 0$ . For y-direction, the origin is located at  $y_C$  and  $y_E$ . Since the

spring constant for  $F_0 = 0$ , it becomes automated to control the constant parameter. By operating in full swing, the system becomes unbalanced. The origin point of  $\theta_H$  and  $\theta_F$  as in balance parameters can be defined as an initial position at  $t = 0$ . Finally, an equilibrium condition occurred when  $\theta_a = \delta_c = 0$ .

Initial reaction forces for  $F_{x0}$  and  $F_{y0}$  can be expressed as

$$F_0 = F_{y0} \cos \theta_H + F_{x0} \sin \theta_H \quad (4)$$

and

$$0 = F_{x0} \cos \theta_F + F_{y0} \sin \theta_F \quad (5)$$

These two equations are solved and finally the equations are expressed as

$$F_{x0} = \frac{-\sin \theta_F \cdot F_0}{(\cos \theta_F \cos \theta_H - \sin \theta_F \sin \theta_H)} \quad (6)$$

Reaction force acting at x- and y-direction can be written as

$$F_{x0} = \frac{-\sin \theta_F}{\cos(\theta_H + \theta_F)} F_0 \quad (7)$$

and

$$F_{y0} = \frac{\cos \theta_F}{\cos(\theta_H + \theta_F)} F_0 \quad (8)$$

Force acting at the x-direction is not equal to zero,  $F_{x0} \neq 0$  when  $\theta_F \neq 0$ . The summation of force in this direction can be written as

$$m_x \ddot{x}_A + c_x (\dot{x}_A + \dot{y}_A \tan \theta_H - \dot{x}_B) + k_x (x_A + y_A \tan \theta_H - x_B) + F_{x0} = 0 \quad (9)$$

And the summation of force in y-direction is

$$m_y \ddot{y}_A + c_y (\dot{y}_A - \dot{y}_C) + \{c_x (\dot{x}_A + y_A \tan \theta_H - \dot{x}_B) + k_x (x_A + y_A \tan \theta_H - x_B)\} \tan \theta_H - F_{y0} = 0 \quad (10)$$

where  $F_{y0} = F_y + k_y (y_A - y_M)$

The condition of  $x_A$  and  $y_M$  can be derived as

$$x_A = x_C + b, \dot{x}_A = \dot{x}_C + \dot{b}, \ddot{x}_A = \ddot{x}_C + \ddot{b}$$

and

$$y_M = y_C + h, \dot{y}_M = \dot{y}_C + \dot{h}, \ddot{y}_M = \ddot{y}_C + \ddot{h}$$

The condition and dependence of  $\theta_a$  and  $\delta_c$ ,  $b$  and  $h$  in a condition of  $A$  based on Table 1 can give a nonlinear equation as follows

$$b = l \left\{ \sin \varphi + \left( \frac{\theta_a}{\kappa} \right) \cos \varphi \right\}$$

$$\dot{b} = l \dot{\theta}_a \left\{ \left( 1 + \frac{1}{\kappa} \right) \cos \varphi - \left( \frac{\theta_a}{\kappa} \right) \sin \varphi \right\}$$

$$\ddot{b} = l \ddot{\theta}_a \left\{ \left( 1 + \frac{1}{\kappa} \right) \cos \varphi - \left( \frac{\theta_a}{\kappa} \right) \sin \varphi \right\} + l \dot{\theta}_a^2 \left\{ \left( 1 + \frac{2}{\kappa} \sin \varphi + \left( \frac{\theta_a}{\kappa} \right) \cos \varphi \right) \right\}$$

and

$$h = l \left\{ \cos \varphi - \left( \frac{\theta_a}{\kappa} \right) \sin \varphi \right\}$$

$$\dot{h} = -l \dot{\theta}_a \left\{ \left( 1 + \frac{1}{\kappa} \right) \sin \varphi + \left( \frac{\theta_a}{\kappa} \right) \cos \varphi \right\}$$

$$\ddot{h} = -l \ddot{\theta}_a \left\{ \left( 1 + \frac{1}{\kappa} \right) \sin \varphi + \left( \frac{\theta_a}{\kappa} \right) \cos \varphi \right\} - l \dot{\theta}_a^2 \left\{ \left( 1 + \frac{2}{\kappa} \cos \varphi - \left( \frac{\theta_a}{\kappa} \right) \sin \varphi \right) \right\}$$

At B condition, the involved equations are

$$b = \delta_c \cos \varphi + l \sin \varphi, \quad \dot{b} = \dot{\delta}_c \cos \varphi, \quad \ddot{b} = \ddot{\delta}_c \cos \varphi$$

and

$$h = -\delta_c \sin \varphi + l \cos \varphi, \quad \dot{h} = -\dot{\delta}_c \sin \varphi, \quad \ddot{h} = -\ddot{\delta}_c \sin \varphi$$

The  $\theta_G$  can be expressed as an explicit function of  $x_A$ ,  $\dot{\theta}_G$  and it follows by

$$\dot{\theta}_G = \theta_G \dot{x}_A \tag{11}$$

where

$$\theta_G = \frac{d\theta_G}{dx_A}$$

By applying the distance between windshield and rubber contact surface,  $h_e$  the equation can be expressed as

$$h_e = l \theta_G \sin \varphi$$

and

$$\dot{h}_e = l(\theta_G \dot{x}_A \sin \varphi + \theta_G \dot{\theta}_a \cos \varphi) \quad (12)$$

The general equation of advanced analytical model at rubber contact surface can be written as

$$\dot{y}_E = \left( \frac{dy_E}{dx_A} \right) \dot{x}_A = \theta_G \dot{x}_A \quad (13)$$

Then, the general equation for distance between windshield and rubber contact surface are

$$y_C = y_E - l\theta_G \sin \varphi$$

and

$$\dot{y}_C = \dot{y}_E - \dot{h}_e = (\theta_G - l\theta_G' \sin \varphi) \dot{x}_A - l\theta_G \dot{\theta}_a \cos \varphi \quad (14)$$

For AC condition, the derivation of 2D advanced mathematical model is described. Firstly, the initial position of arm and blade is referred from Figure 1, the equation in x-direction can be written as

$$m_x \ddot{x}_A + c_x (\dot{x}_A + \dot{y}_A \tan \theta_H - \dot{x}_B) + k_x (x_A + y_A \tan \theta_H - x_B) + F_{x0} = 0 \quad (15)$$

By taking a condition of  $x_A$  and substitute into Eq. (15), the new equation can be described as

$$m_x (\ddot{x}_C + \ddot{b}) + c_x ((\dot{x}_C + \dot{b}) + \dot{y}_A \tan \theta_H - \dot{x}_B) + k_x ((x_C + b) + y_A \tan \theta_H - x_B) + F_{x0} = 0 \quad (16)$$

By using the equation of reaction forces and the substituting it into Eq. (16), the equation become

$$m_x (\ddot{x}_C + \ddot{b}) + c_x ((\dot{x}_C + \dot{b}) + \dot{y}_A \tan \theta_H - \dot{x}_B) + k_x ((x_C + b) + y_A \tan \theta_H - x_B) = \frac{\sin \theta_F}{\cos(\theta_H + \theta_F)} F \quad (17)$$

For y-direction, the equation can be written as

$$\ddot{x}_A = l\ddot{\theta}_a \left\{ \left( 1 + \frac{1}{\kappa} \right) \cos \varphi - \left( \frac{\theta_a}{\kappa} \right) \sin \varphi \right\} - \dot{\theta}_a^2 \left\{ \left( 1 + \frac{2}{\kappa} \right) \sin \varphi + \left( \frac{\theta_a}{\kappa} \right) \cos \varphi \right\} \quad (18)$$

Based on condition at  $y_M$ ,  $h$  and  $y_c$  the Eq. (18) can be simplified as a

$$y_M = y_E + l \left\{ \cos \varphi - \left( \theta_G + \frac{\theta_a}{\kappa} \right) \sin \varphi - \cos \theta_F + \theta_{G0} \sin \theta_F \right\} \quad (19)$$

According to relationship x- and y-direction reaction forces, Eq. (19) can be expanded as

$$F_x = \frac{1}{\cos \varphi} \times [AA_1 [AA_2 \{AA_3\} - AA_4]] \quad (20)$$

where

$$AA_1 = \frac{k_a \theta_a}{l} + k_y \sin \varphi$$

$$AA_2 = y_A - y_E - l$$

$$AA_3 = \cos \varphi - \left( \theta_G + \frac{\theta_a}{\kappa} \right) \sin \varphi - \cos \theta_F$$

and

$$AA_4 = F_{y0} \sin \varphi$$

At  $F_{x0} \neq 0$  and  $\theta_F \neq 0$ , Eq. (20) is become

$$m_x l \ddot{\theta}_a \cos \varphi \left\{ \left( 1 + \frac{1}{\kappa} \right) \cos \varphi - \left( \frac{\theta_a}{\kappa} \right) \right\} - m_x l \dot{\theta}_a^2 \cos \varphi \left\{ \left( 1 + \frac{2}{\kappa} \right) \sin \varphi + \left( \frac{\theta_a}{\kappa} \cos \varphi \right) \right\} + \frac{k_a \theta_a}{l} \dots$$

$$\dots + \cos \varphi \{ c_x (\dot{x}_A + \dot{y}_A \tan \theta_H - \dot{x}_B) + AA_5 \} + k_y \sin \varphi \times [y_A - y_E - l \{ AA_6 \}] - F_{y0} \sin \varphi = 0 \quad (21)$$

where

$$AA_5 = k_x (x_A + y_A \tan \theta_H - x_B)$$

and

$$AA_6 = \cos \varphi - \left( \theta_G + \frac{\theta_a}{\kappa} \right) \sin \varphi - \cos \theta_F + \theta_{G0} \sin \theta_F$$

By taking a condition of  $x_A$  and substitute into Eq. (21), the equation can be simplified to

$$m_y \ddot{y}_A + c_y \dot{y}_A + \left[ y_A - y_E - l \left\{ \theta_G + \frac{\theta_a}{\kappa} \sin \varphi - \cos \theta_F + \theta_{G0} \sin \theta_F \right\} \right] \dots \quad (22)$$

$$\dots + \tan \theta_H \times \{ c_x (\dot{x}_A + \dot{y}_A \tan \theta_H - \dot{x}_B) + k_x (x_A + y_A \tan \theta_H - x_B) \} = 0$$

where

$$x_A = x_C + l \left\{ \sin \varphi + \left( \frac{\theta_a}{\kappa} \right) \cos \varphi \right\} \quad (23)$$

and

$$\dot{x}_A = l \dot{\theta}_a \left\{ \left( 1 + \frac{1}{\kappa} \right) \cos \varphi - \left( \frac{\theta_a}{\kappa} \right) \sin \varphi \right\} \quad (24)$$

By integrating Eqs. (22), (23) and (24), the adopt variables are  $(\theta_a, \dot{\theta}_a, \ddot{\theta}_a)$  and  $(y_a, \dot{y}_a, \ddot{y}_a)$  which are the constant values. All equations for y-direction can be simplified as



$$m_y \ddot{y}_A + c_y (\dot{y}_A - \dot{y}_C) + \{c_x (\dot{x}_A + \dot{y}_A \tan \theta_H - \dot{x}_B) + k_x (x_A + y_A \tan \theta_H - x_B)\} \times \dots \quad (25)$$

$$\dots \tan \theta_H - F_{y0} = 0$$

where  $y_A = y_M$  is the neck rotation centre position for free length of spring and  $k_y$  is a spring constant at y-direction.  
 Then,

$$F_{y0} = \frac{\cos \theta_F}{\cos(\theta_H + \theta_F)} F_0 \quad (26)$$

where  $\theta_F$  is the arm front twist angle,  $\theta_H$  is arm head twist angle and  $F_0$  is arm pressure.

By simplifying Eqs. (25) and (26), the equation becomes

$$y_M = y_E + l \left\{ \cos \varphi - \left( \theta_G + \frac{\theta_a}{\kappa} \right) \sin \varphi - \cos \theta_F + \theta_{G0} \sin \theta_F \right\} \quad (27)$$

where  $y_E = \theta_G \cdot x_A$  which,  $\theta_G$  is a windshield glass profile and  $x_A$  is a horizontal displacement at  $k_y$ .

Then, horizontal displacement equation can be written as

$$x_A = x_C + l \left\{ \sin \varphi + \left( \frac{\theta_a}{\kappa} \right) \cos \varphi \right\} \quad (28)$$

where  $\varphi = \theta_a + \theta_F$  which,  $\theta_a$  is rotational angle of rubber neck and  $\theta_F$  is arm front twist angle, particularly.

Then,  $\kappa = l^2 k_c / k_a$  and  $x_C = 0$ . Vertical displacement of rubber blade can be obtained as a

$$\dot{y}_C = \dot{y}_E - \dot{h}_e = (\theta_G - l \theta_a \sin \varphi) \dot{x}_A - l \theta_G \dot{\theta}_a \cos \varphi \quad (29)$$

where

$$\dot{x}_A = l \dot{\theta}_a \left\{ \left( 1 + \frac{1}{\kappa} \right) \cos \varphi - \left( \frac{\theta_a}{\kappa} \right) \sin \varphi \right\}$$

Finally, 2-D advanced mathematical model for y-direction can be expressed as

$$m_y \ddot{y}_A + c_y (\dot{y}_A - \dot{y}_C) + \{c_x (AA_7) + k_x (x_A + y_A \tan \theta_H - x_B)\} \tan \theta_H \dots \quad (30)$$

$$\dots - F_y + F_{y0} = 0$$

where

$$AA_7 = \dot{x}_A + \dot{y}_A \tan \theta_H - \dot{x}_B$$

By simplifying Eq. (29), it is become

$$m_y \ddot{y}_A + c_y \left[ \dot{y}_A - \left( \theta_G - l \theta_G \sin \varphi \right) \dot{x}_A - l \theta_G \dot{\theta}_a \cos \varphi \right] + k_x (AA_8 + AA_9) + k_x (AA_{10} \times AA_{11}) \dots \quad (31)$$

$$\dots - (AA_{12} + AA_{13}) = 0$$

where

$$AA_8 = l \dot{\theta}_a \left( 1 + \frac{1}{\kappa} \right) \cos \varphi - \left( \frac{\theta_a}{\kappa} \right) \sin \varphi$$

$$AA_9 = \dot{y}_A \tan \theta_H - \dot{x}_B$$

$$AA_{10} = x_c + l \left\{ \sin \varphi + \left( \frac{\theta_a}{\kappa} \right) \cos \varphi \right\} + y_A \tan \theta_H - x_B$$

$$AA_{11} = \tan \theta_H$$

$$AA_{12} = -k_y (y_A - y_M) + \frac{\cos \theta_F}{\cos(\theta_H - \theta_F)} F_0$$

$$AA_{13} = \frac{\cos \theta_F}{\cos(\theta_H - \theta_F)} F_0$$

Finally, 2-D advanced mathematical for x-direction can be expressed as

$$m_x (\ddot{x}_c + \ddot{b}) + c_x \left( (\dot{x}_c + \dot{b}) + \dot{y}_A \tan \theta_H - \dot{x}_B \right) + k_x \left( (x_c + b) + y_A \tan \theta_H - x_B \right) + F_{x0} = \frac{-\sin \theta_F}{\cos(\theta_H + \theta_F)} F_0 \quad (32)$$

Finally, Eqs (30) and (32) are used to simulate the baseline noise and vibration level of the automotive wiper before implementing the control scheme.

## 2.2 Input Shaping Strategy

Input shaping (IS) vibration control scheme involves convolving desired command in order to develop impulse sequence. It is also known as an input shaper because it produces the shaped system as an input. The main objective of using IS is to calculate the eliminated vibrations at certain amplitude, time location and desire frequency [15, 18-20]. This IS can be made insensitive to make a variation in a resonant frequency. It is more effective to minimize vibration in flexible systems such as automotive vehicles wiper system, that the frequency shifts during moves such as moving component in vehicle. The vibratory system of any order can be modelled as s superposition of second order systems [17,21]. The transfer function can be written as

$$G(s) = \frac{\omega_n^2}{s^2 + 2\xi\omega_n s + \omega_n^2} \quad (33)$$

where  $\omega_n$  is natural frequency and  $\xi$  is damping ratio of the system.

The impulse response can be represented as

$$y(t) = \frac{A\omega_n}{\sqrt{1-\xi^2}} e^{-\xi\omega_n(t-t_0)} \sin\left[\omega_n\sqrt{1-\xi^2}(t-t_0)\right] \quad (34)$$

where  $A$  is an amplitude and  $t_0$  is time of the impulse.

The response of impulses can be represented by the superposition of the impulse response. For  $N$  impulse with  $\omega_d = \omega_n\sqrt{1-\xi^2}$  can be expressed as

$$y(t) = M \sin(\omega_d t + \alpha) \quad (35)$$

where

$$M = \sqrt{\left(\sum_{i=1}^N B_i \cos \Phi_i\right)^2 + \left(\sum_{i=1}^N B_i \cos \theta_i\right)^2}$$

$$B_i = \frac{A_i \omega_n}{\sqrt{1-\xi^2}} e^{-\xi\omega(t-t_i)}$$

$$\Phi_i = \omega_d t_i$$

$$\alpha = \tan^{-1}\left(\frac{\sum_{i=1}^N B_i \cos \Phi_i}{\sum_{i=1}^N B_i \sin \Phi_i}\right)$$

where  $A_i$  is a magnitude and  $t_i$  is a time, respectively.

Then, it is occurred by the impulse response. The residual single mode amplitude of the vibration is based on the impulse response and it can be evaluating at time of the last impulse,  $t_N$ . In equation, it can be written as

$$V = \sqrt{V_1^2 + V_2^2} \quad (36)$$

where

$$V_1 = \sum_{i=1}^N \frac{A_i \omega_n}{\sqrt{1-\xi^2}} e^{-\xi\omega_n(t_N-t_i)\cos(\omega_d t_i)}$$

and

$$V_2 = \sum_{i=1}^N \frac{A_i \omega_n}{\sqrt{1-\xi^2}} e^{-\xi\omega_n(t_N-t_i)\sin(\omega_d t_i)} \quad (37)$$

In order to achieve zero vibration after applying the input, it is required that both  $V_1$  and  $V_2$  in Eq. (36) are directly equal to zero. To ensure that the shaped command input can give the same value of the rigid body motion such as an unshaped command, the summation of the amplitude of impulse must be unity. To avoid delay, first impulse is zero bases on time and value of  $V_1$  and  $V_2$  also set to zero. Thus,

$$\sum_{i=1}^N A_i = 1 \tag{38}$$

And it yields four impulse response sequences with parameters as a

$$t_1 = 0, t_2 = \frac{\pi}{\omega_d}, t_3 = \frac{2\pi}{\omega_d}, t_4 = \frac{3\pi}{\omega_d} \tag{39}$$

The amplitude equation can be expressed as

$$A_1 = \frac{1}{1+3K+3K^2+K^3}, A_2 = \frac{3}{1+3K+3K^2+K^3}$$

$$A_3 = \frac{3K^2}{1+3K+3K^2+K^3}, A_4 = \frac{K^3}{1+3K+3K^2+K^3} \tag{40}$$

where

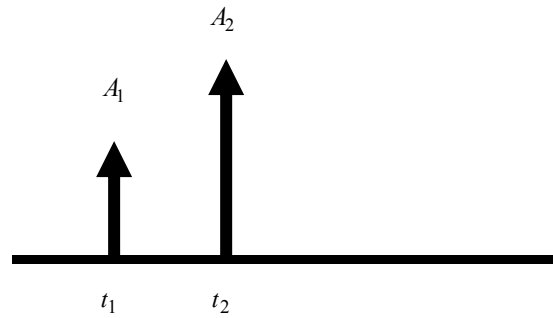
$$K = \frac{-\xi\pi}{e^{\sqrt{1-\xi^2}}}$$

Higher vibration response can be solved when an impulse sequence for each vibration mode is designed independently.

### 2.2.1. Two Impulse

Two impulse sequence input shaper is used to achieve the zero vibration (ZV) after input has reached at the end point, which means it is required that both  $V_1$  and  $V_2$  are independently equal to zero. To ensure the shaped of command input produce the same rigid body motion, it is required to make a summation for a value of amplitude become unity. It is taking a bit of time to complete and produce a delay [22].

First impulse is selected at time  $t_1 = 0$  to avoid the response delay. The value of  $V_1$  and  $V_2$  must be set to zero and satisfying Eq. (38) and finally solved a two impulse sequence as shown in Figure 2.



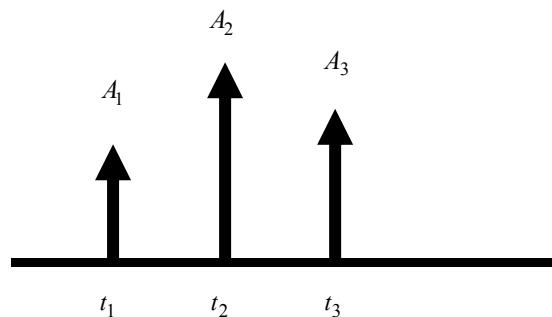
**Figure 2.** Two impulse sequence.

### 2.2.2. Three Impulse

Three impulse sequence is used to generate the robustness of the input shaper to make an error in natural frequencies itself. It can be increased by setting the residual mode amplitude to

$$\frac{dV}{d\omega_n} = 0 \quad (41)$$

By setting the derivative to zero, the system is equivalent to produce small changes in vibration correspond to a natural frequency changes [22]. By using Eq. (36), then it can be simplified by Singer and represented by Eq. (37). The three impulse sequence finally can be represented in Figure 3.

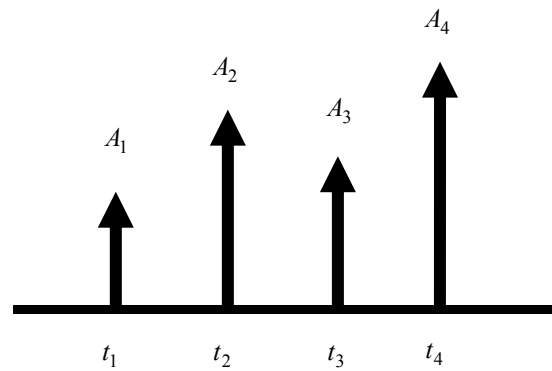


**Figure 3.** Three impulse sequence.

### 2.2.3. Four Impulse

By using four impulse sequence in input shaper, the robustness is slightly increased by solving the second derivative of the impulse response shown in Eq. (33). The higher vibration mode of nonlinear system can be handling easily by using this sequence. Impulse sequence for each vibration modes is independently designed. It can be used together such as a form of impulse sequence which is attenuated the vibration at higher modes [22].

For nonlinear system, higher vibration amplitude can be reduced by accomplishing the system with four impulses. Figure 4 shows the four impulse sequence schematic diagram for input shaper.

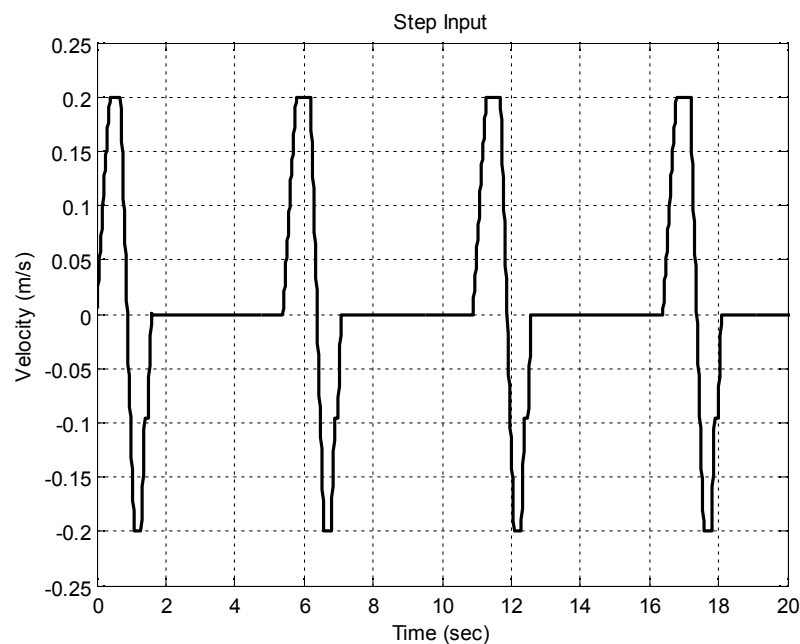


**Figure 4.** Four impulse sequence.

### 3. RESULTS AND DISCUSSION

#### 3.1. Baseline Prediction Model

In this study, input data are required to simulate the 2D mathematical model. Step input represents the source data into to the system during operation. The time range is approximate to 20 s and the velocity range is between -0.25 to 0.25 m/s, where it represents the up and down velocity. Figure 5 shows the step input applied in this study.

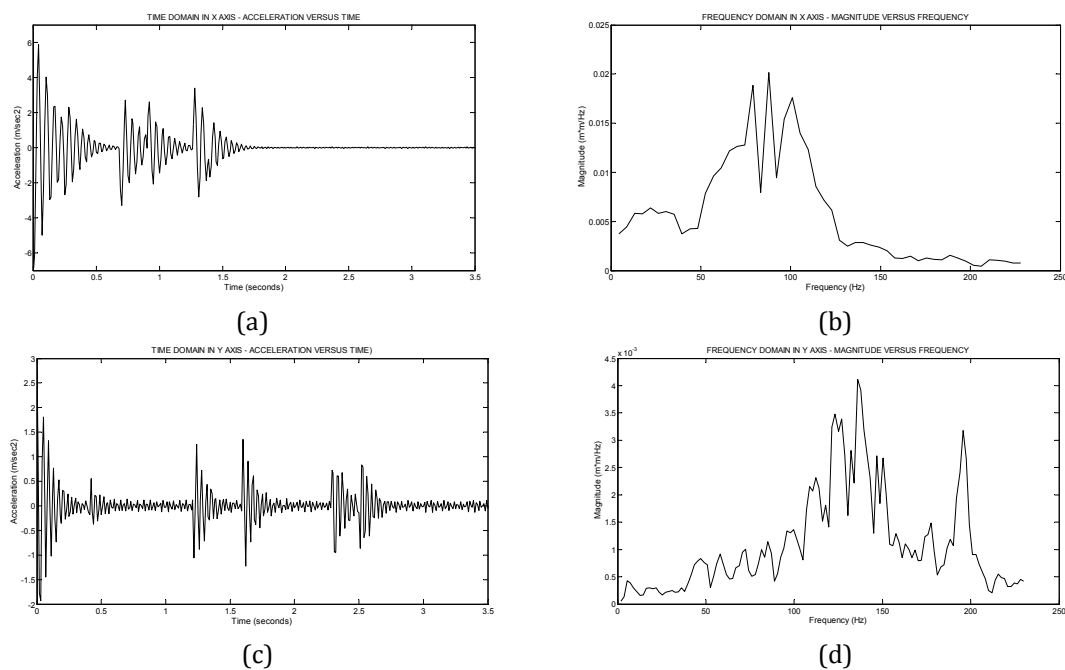


**Figure 5.** Step input.

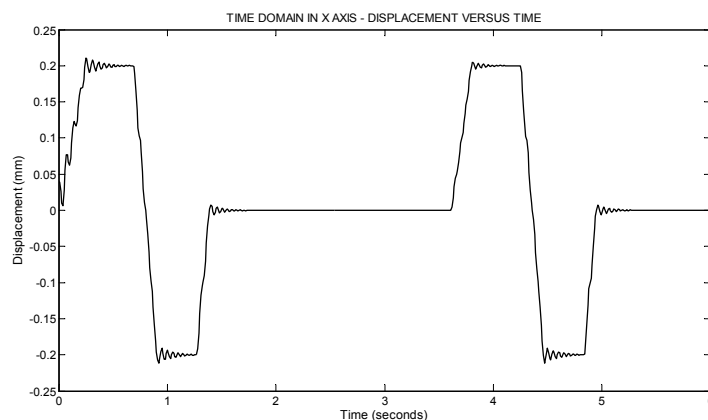
The result represents in time, frequency and stick-slip condition. Time and frequency domain represent the variety of unwanted noise and vibration. The maximum rates of unwanted noise are  $4.3 \text{ m/s}^2$  and  $1.5 \text{ m/s}^2$  for x- and y-direction, respectively. In frequency domain, the highest frequency is recorded at  $0.02 \text{ m.m/Hz}$  which is located at  $92.72 \text{ Hz}$  and shows the unwanted vibration occurred at x-direction. For y-direction, the unwanted vibration occurred at  $4.2 \times 10^{-3} \text{ m.m/Hz}$  and located at  $128.2 \text{ Hz}$ . All of the results have been shown in Figure 6.

The stick-slip conditions signify the behaviour of the rubber blade contact with windscreen and only happen at x-direction. This condition occurred due to contact stress and strains were obtained the rubber blade during the operation. It greatly affects the residual stress and residual shear strain within a thin layer of the material near to the contact surface of windscreen. Residual stress in this direction is not significantly influenced by y-direction. The pattern of the stick-slip results is slightly equivalent in step input diagram because the effect condition is proportional to the input. The different shape is happened at point -0.2 and -0.2 mm where the shape is alike as sinusoidal shape and shows in Figure 7.

The jump condition only occurred at y-direction. It is happened due to the extraneous objects which have been attached in rubber blade. This extraneous exists in the edge of the rubber blade. It can adopt the potential effect to produce the jump condition. In the other hands, it is occurred where the wiper blade does not have the capability of moving efficiently across the windscreen surface. It can create a noisy sound and bounces, consequently, causing discomfort to driver and passengers. The result shows in Figure 8.



**Figure 6.** Results of unwanted noise and vibration for x- and y-direction (a) time domain at x-direction, (b) frequency domain at x-direction, (c) time domain at y-direction and (d) frequency domain at y-direction.



**Figure 7.** Stick-slip condition.

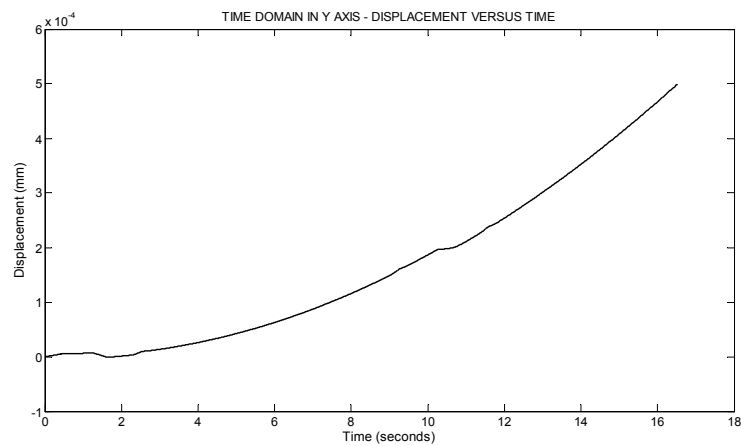


Figure 8. Jump condition.

### 3.2. Verification with Finite Element Models

Finite Element Method (FEM) is another method used for investigation of unwanted noise and vibration in wiper system. The verification of 2D mathematical model with FEM is necessary before making further analysis. The FEM results were adopted from Awang and shown in Figure 9 [18]. Then, verification results between baseline and FEM was made and shown in Figure 10.

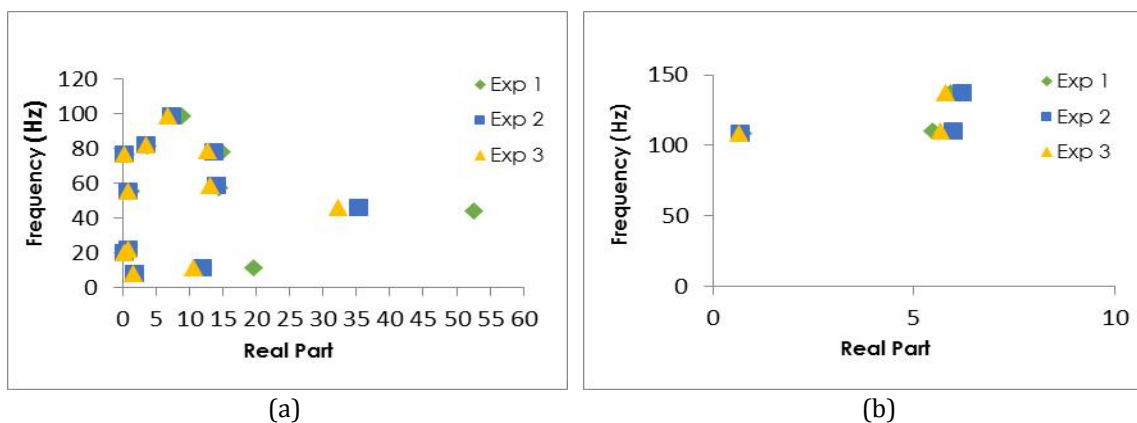


Figure 9. Finite element results (a) x-direction and (b) y-direction.

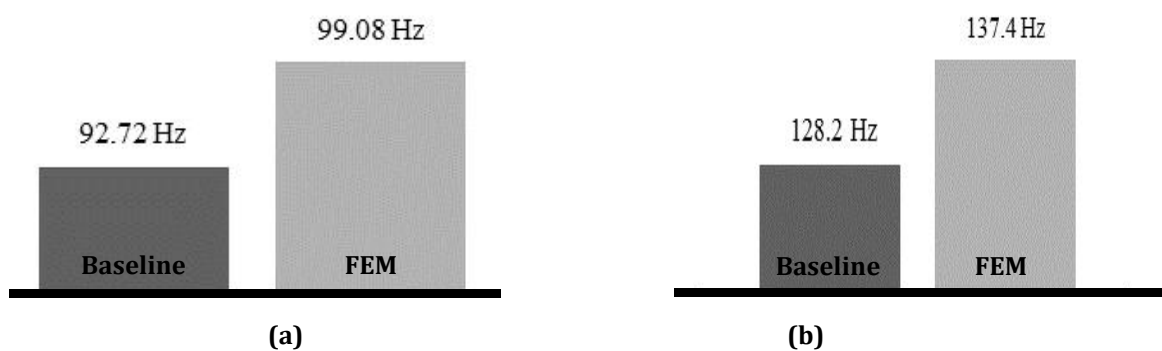


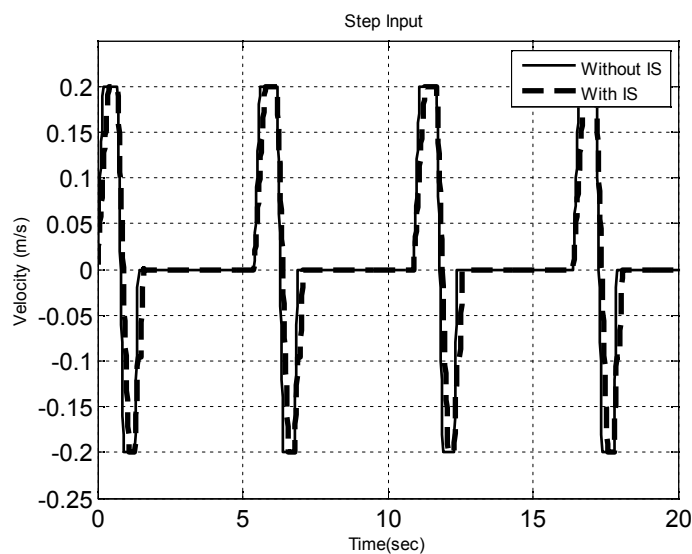
Figure 10. Verification results (a) x-direction and (b) y-direction.



### 3.3. Prediction Results using Input Shaping Strategy

In Figure 11, the step input with and without implementation of IS scheme. Shape of the graph changed after applying the IS. This scheme moves a bit from the time shaped in initial shaped produced by the step input. The desired period of step input is to be as small as possible as at delays time between one complete cycles of input. Time delay can produce low frequency of step input and can affect the response of wiper system. The advantages of IS scheme, it is a feed forward control method and has a potential to reduce vibration in flexible structure [23-26]. IS scheme being a method in which creates a command signal to cancel out the unwanted vibration amplitude and it is called as self-turning technique. By using this self-turning, the vibration at first part of the system is cancel out by second part of the command.

For x- and y-directions, the comparison result is shown in Table 2. The result indicates that IS scheme has given better improvement in reducing the range of noise and vibration for both directions.



**Figure 11.** Step input with and without implementation of IS strategy.

**Table 2** Comparison for x- and y-direction with and without implementation of input shaping strategies

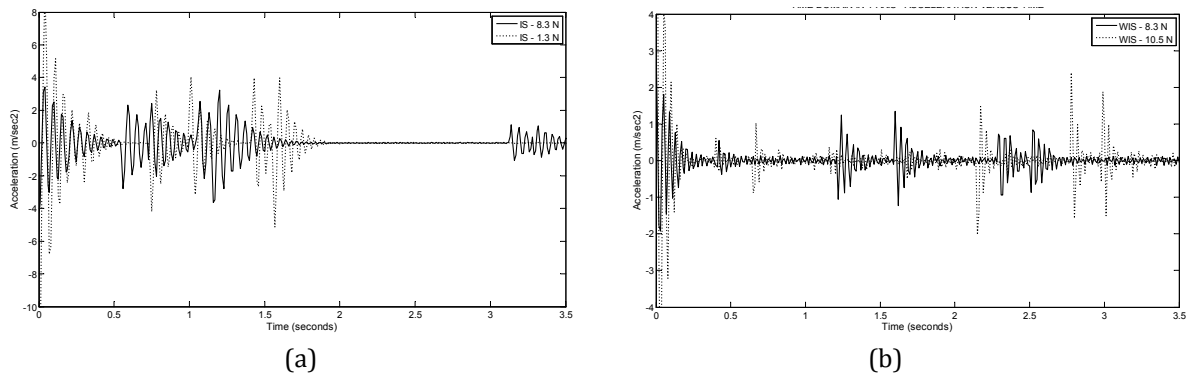
	x-direction	y-direction
<b>Noise:</b>		
Without input shaping	4.3 m/s <sup>2</sup>	1.5 m/s <sup>2</sup>
With input shaping	3.7 m/s <sup>2</sup>	1.3 m/s <sup>2</sup>
<b>Vibration:</b>		
Without input shaping	0.02 m.m/Hz	4.2 x 10 <sup>-3</sup> m.m/Hz
With input shaping	0.015 m.m/Hz	2.7 x 10 <sup>-3</sup> m.m/Hz
<b>Stick-Slip:</b>		
Without input shaping	No time delay	None
With input shaping	Time delay	None
<b>Jump:</b>		
Without input shaping	None	24.77 s
With input shaping	None	24.67

### 3.4. Parametric Evaluation

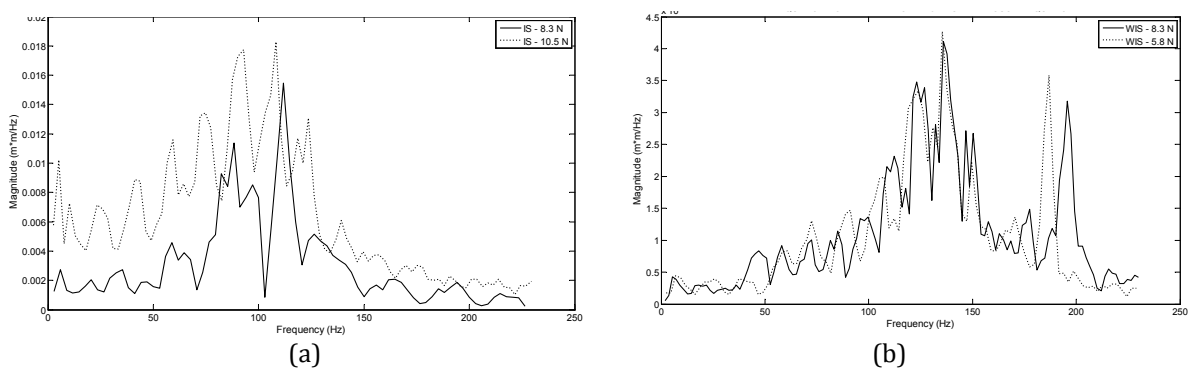
The selection of parameter is entirely difficult because the selection is somewhat arbitrary. The selected parameters are force, friction and contact angle. The initial values of these parameters are 8.3 N, 0.3 and 16 deg. These initial values then modified by using try and error method to reduce the unwanted noise and vibration in wiper system. The range of the modification values are between 1.3 to 10.5 N, 0.11 to 0.56 and 9 to 18.5 deg. This range is based on the minimum and maximum values for wiper system during the operation. For force parameter, the sample results are shown in Figures 12 and 13 for both x- and y-direction. The effectiveness values to reduce unwanted noise are 4.7, 5.8 and 10.5 N and unwanted vibration is increased when applied the same value.

For friction, there are four values that been chosen and believe can reduce the unwanted noise but unfortunately it slightly increased the unwanted vibration level. The values are 0.17, 0.26, 0.42 and 0.56. The sample results for both directions are shown in Figures 14 and 15.

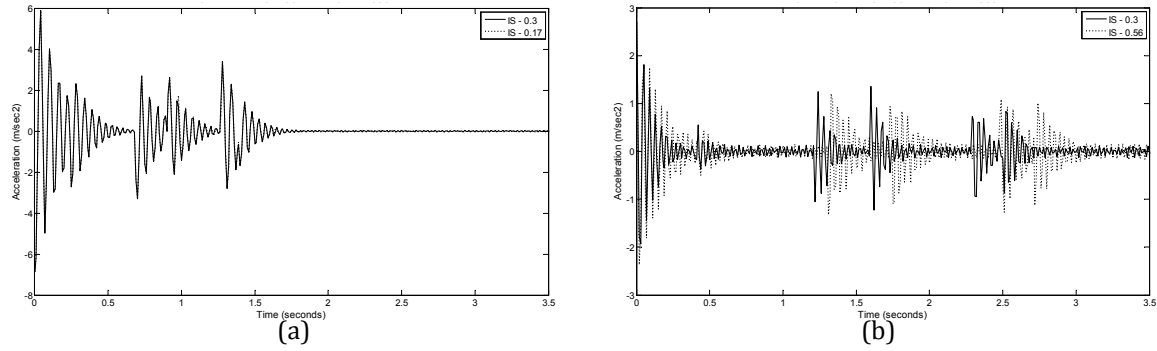
In contact angle analysis, the effectiveness range is between 9.4 to 18.5 deg. The results are shown in Figures 16 and 17 for both x- and y-direction, respectively.



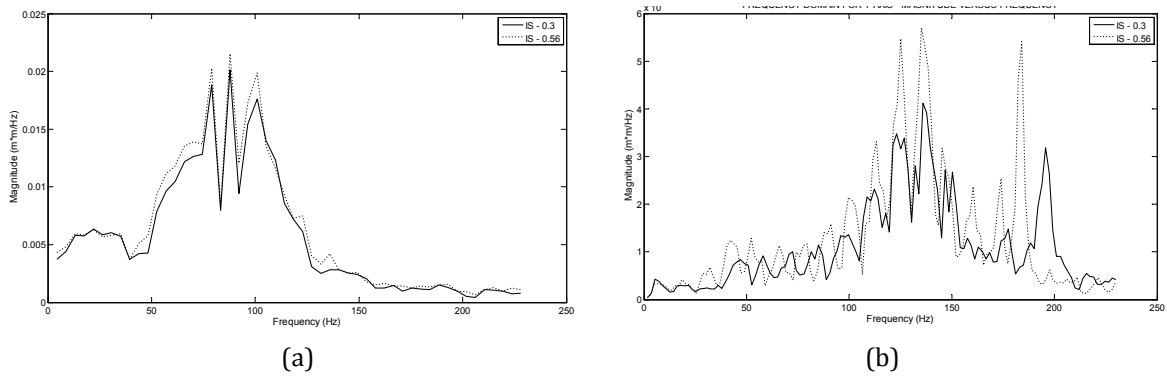
**Figure 12.** Results for unwanted noise by applying force parameter (a) x- and (b) y-direction.



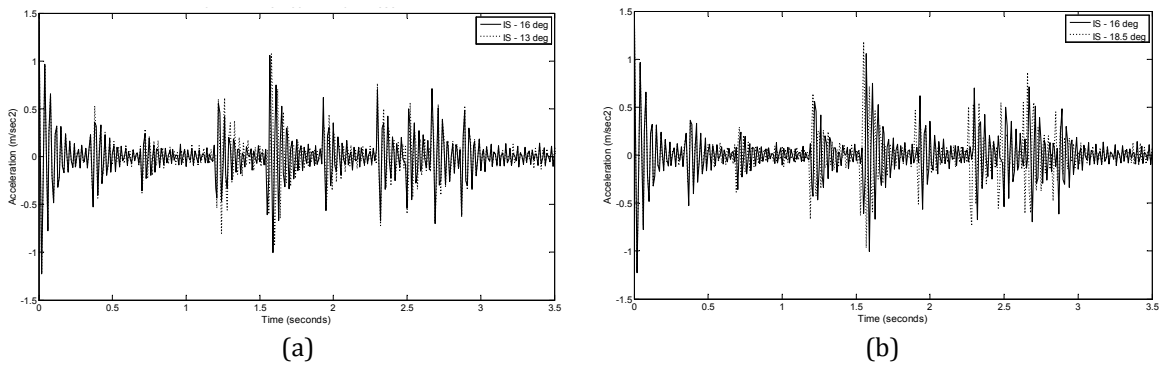
**Figure 13.** Results for unwanted vibration by applying force parameter (a) x- and (b) y-direction.



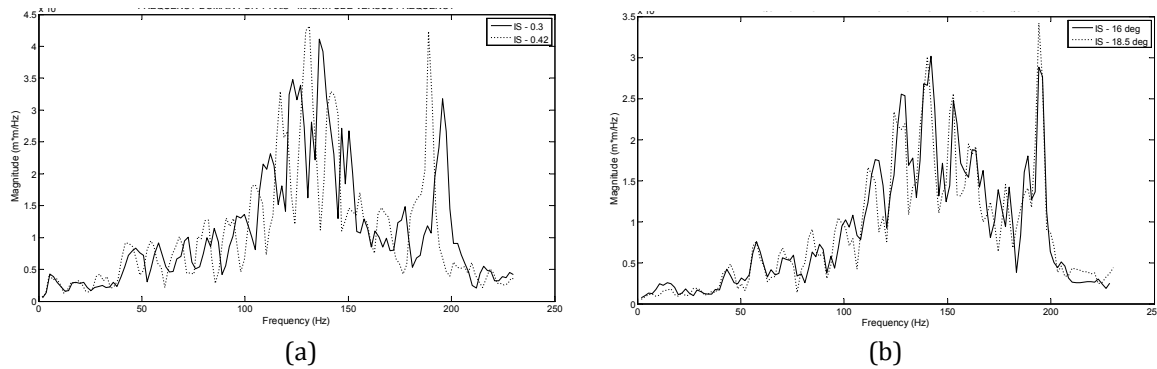
**Figure 14.** Results for unwanted noise scheme by applying friction parameter (a) x- and (b) y-direction.



**Figure 15.** Results for unwanted vibration by applying friction parameter (a) x- and (b) y-direction.



**Figure 16.** Results for unwanted noise by applying contact angle parameter (a) x- and (b) y-direction.



**Figure 17.** Results for unwanted vibration by applying contact angle parameter (a) x- and (b) y-direction.

Based on the results given, these three parameters have an agreement to reduce unwanted noise and vibration in wiper system.

#### 4. CONCLUSION

This study modelled the governing equation of wiper blade system. Noise and vibration response of the wiper blade in the vertical (y-direction) and longitudinal (x-axis) were monitored. Input shaping vibration control scheme was applied to enhance the level of unwanted noise and vibration generated by the wiper blade system, and the results were compared with the baseline results, which did not have any control scheme applied to the wiper blade system. Additionally, parameter studies were also involved to monitor the unwanted noise and vibration level. Several number of parameters such as force, friction and contact angle had been chosen, and finally, the level of unwanted noise and vibration was successfully reduced. This approach can be used as prediction tool that was limited to linear model.

#### ACKNOWLEDGEMENTS

Special thanks to the Advanced Academia-Industry Collaboration Laboratory (AiCL) and Fakulti Kejuruteraan Mekanikal (FKM), Universiti Teknikal Malaysia Melaka (UTeM) for providing the laboratory facilities.

#### REFERENCES

- [1] Okura, S., Sekiguchi, T., & Oya, T., "Dynamic analysis of blade reversal behavior in a windshield wiper system", No. 2000-01-0127, (2000) SAE Technical Paper.
- [2] Salim, M. A., Zain, M. M., Bakar, A. A., Mat, S., & Rahman, M. N., "The application of input shaping scheme for arm force in automotive wiper blade", In International Conference on Instrumentation, Control & Automation, Bandung, Indonesia, (2009).
- [3] Salim, M. A., Noordin, A., Munir, F. A., & Nuri, N. R. M., "The relationship of contact angle and input shaping scheme in automotive wiper system", In Computing and Communication Technologies, Research, Innovation, and Vision for the Future (RIVF), 2012 IEEE RIVF, (2012) pp.1-4).
- [4] Grenouillat, R., & Leblanc, C., "Simulation of mechanical pressure in a rubber-glass contact for wiper system", SAE Paper, 01-0798, 2002.
- [5] Salim, M. A., Noordin, A., Zain, M. M., & Bakar, A. A., "The analysis of friction effect in automotive wiper system using input shaping technique", In Proceedings of the World Congress on Engineering, (2010).

- [6] Goto, S., Takahashi, H., & Oya, T., "*Investigation of wiper blade squeal noise reduction measures*", No. 2001-01-1410, (2001), SAE Technical Paper.
- [7] Koenen, A., & Sanon, A., "*Tribological and vibroacoustic behavior of a contact between rubber and glass (application to wiper blade)*", Tribology International, **40** (10-12), (2007) pp.1484-1491.
- [8] Chang, S. C., & Chen, S. C., "*Dither signals with particular application to the control of windscreen wiper blades*", International journal of solids and structures, **43**(22-23), (2006) pp.6998-7013.
- [9] Stallaert, B., Doucet, F., Rys, J., Diallo, A., Chaigne, S., Swevers, J., & Sas, P., "*Application of dither control for automotive wiper squeal*", In Proceedings of ISMA, (2006) pp. 263-272.
- [10] Shoda, H., & Amagasa, T., U.S. Patent Application No. 15/127,047, 2017.
- [11] Viscardi, M., Leo, R., Ciminello, M., & Brandizzi, M., "*Preliminary experimental/numerical study of the vibration annoyance control of a windshield wiper mechanical system through a Synchronized Switch Shunt Resonator (SSSR) technology*", Journal of Theoretical and Applied Mechanics, **56** (2018).
- [12] Chen, T. J., & Hong, Y., "*Geometric analysis of the vibration of rubber wiper blade*", Taiwanese Journal of Mathematics, **1**(1), (2021) pp.1-26.
- [13] Haijima, T., Aiuchi, K., & Uchiyama, N., "*Optimal motion trajectory generation for automotive windshield wiper systems using the response surface method*", In 2020 IEEE/SICE International Symposium on System Integration (SII), (2020) pp.567-572, IEEE.
- [14] Reniers, M., & Thuijsman, S., "*Supervisory control for dynamic feature configuration in product lines*", In 2020 Forum for Specification and Design Languages (FDL), (2020) pp.1-8, IEEE.
- [15] Singer, N., Singhose, W., & Kriekku, E., "*An input shaping controller enabling cranes to move without sway*", In ANS 7th topical meeting on robotics and remote systems, **1**, (1997) pp.225-31.
- [16] Huang, M., "*Analysis of friction induced stability, bifurcation, chaos, stick-slip vibration and their impacts on wiping effect of automotive wiper system*", SAE International Journal of Passenger Cars-Mechanical Systems, **7** (2014-01-0021), (2014) pp.21-31.
- [17] Lancioni, G., Lenci, S., & Galvanetto, U., "*Dynamics of windscreen wiper blades: Squeal noise, reversal noise and chattering*", International Journal of Non-Linear Mechanics, **80**, (2016) pp.132-143..
- [18] Awang, I. M., Leong, C. Y., Abu-Bakar, A. R., Abd-Ghani, B., Abd-Rahman, R., & Md-Zain, M. Z., "*Modeling and simulation of automotive wiper noise and vibration using finite element method. Evaluation of an Automotive Wiper Noise and Vibration Characteristics using Numerical Approach*", **13**, (2009).
- [19] Pao, L. Y., & Lau, M. A., "*Robust input shaper control design for parameter variations in flexible structures*", Journal of dynamic systems, measurement, and control, **122**(1), (2000) pp.63-70.
- [20] Salim, M. A., Abdullah, M. A., Noordin, A., Jusoff, K., & Zin, M. Z., "*Modeling, simulation and verification of parameters study on flexible automotive wiper*", Advanced Science Letters, **19**(1), (2013) pp.106-112.
- [21] Unno, M., Shibata, A., Yabuno, H., Yanagisawa, D., & Nakano, T., "*Analysis of the behavior of a wiper blade around the reversal in consideration of dynamic and static friction*", Journal of Sound and Vibration, **393**, (2017) pp.76-91.
- [22] Zain, M. Z. M., Mailah, M., & Priyandoko, G. P. G., "*Active force control with input shaping technique for a suspension system*", Jurnal Mekanikal, **27**(2), (2008).
- [23] Lee, S. H., Kim, Y. H., Sung, J., Shin, K. C., & Oh, J. H., "*Investigation of the contact force distribution and dynamic behaviour of an automobile windshield wiper blade system*", Proceedings of the Institution of Mechanical Engineers, Part D: Journal of Automobile Engineering, **227**(7), (2013) pp.1040-1052.

- [24] Salim, M. A., Munir, F. A., & Noordin, A., "*Experimental study on vibration level of automotive flexible wiper system*", *Journal of Engineering and Technology*, **3**, (2012) pp.123-138.
- [25] Shreya, V. S., & Balaji, P., "*Design of synchronous controller for the application of intelligent locomotive wipers*," *Journal of Electrical Systems*, **1**(1), (2020) pp.1-8.
- [26] Zolfagharian, A., Noshadi, A., Khosravani, M. R., & Zain, M. Z. M., "*Unwanted noise and vibration control using finite element analysis and artificial intelligence*", *Applied Mathematical Modelling*, **38**(9-10), (2014) pp.2435-2453.